



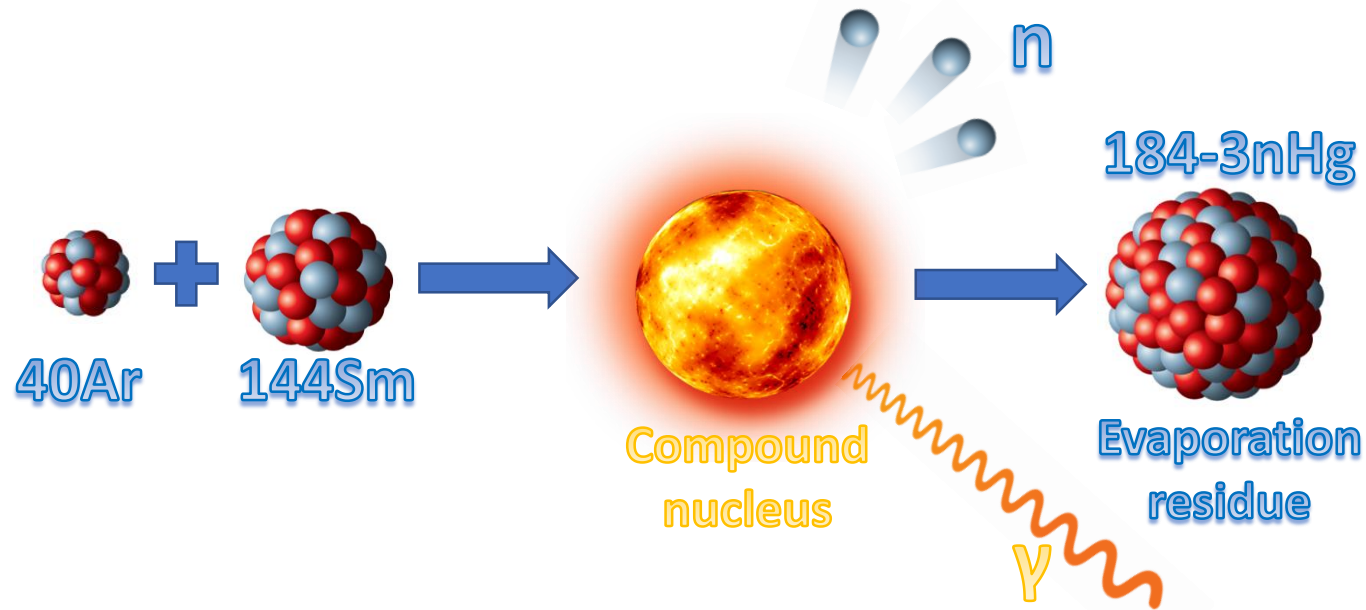
*Flerov Laboratory of Nuclear Reactions
JINR, Dubna, Russia
Sector №4 (MASHA)*

*Mgr. Antonín Opíchal
Palacký University in Olomouc
Applied Physics*



Data analysis from catcher foil experiment for cross sections
measurement of $^{40}\text{Ar}+^{144}\text{Sm}$ reaction

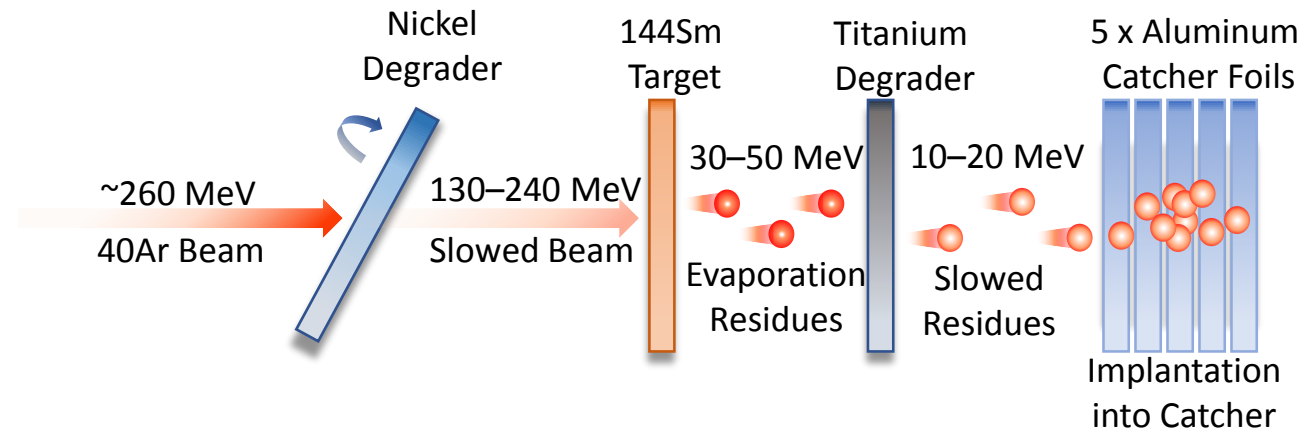
Hot Fusion Reaction



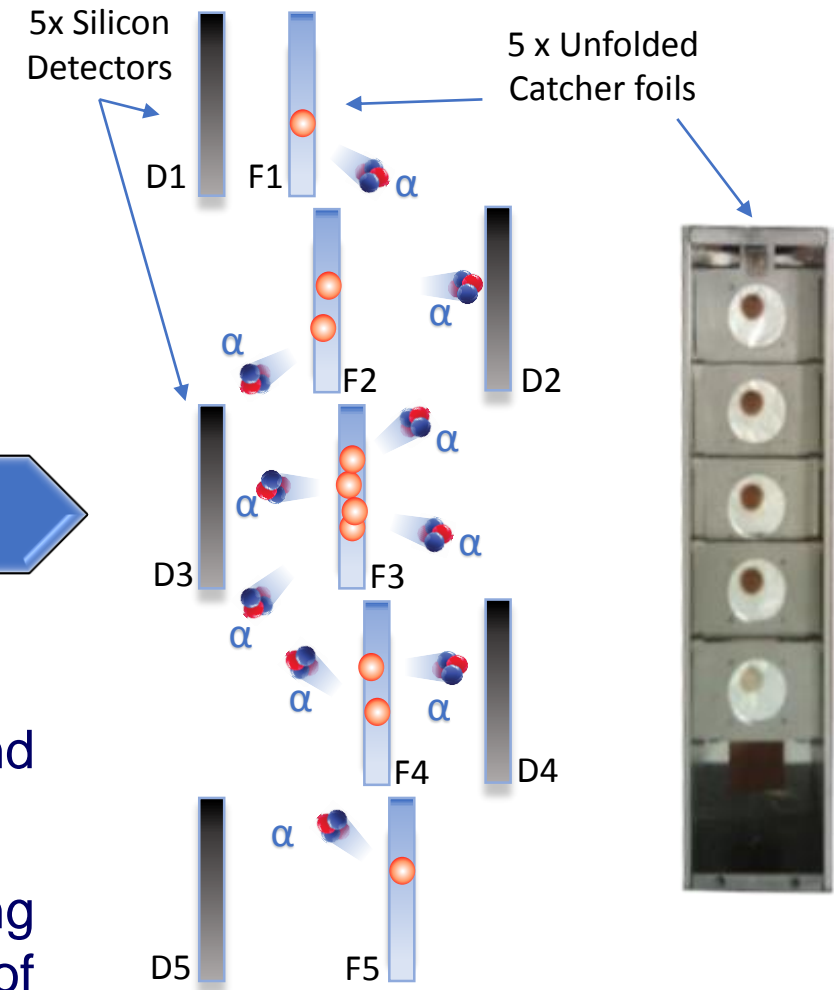
- An ^{40}Ar ion beam from cyclotron U400M irradiated a ^{144}Sm fixed target
- Complete fusion reaction lead to compound nucleus formation
- The compound nucleus is in highly excited state (so-called *Hot Fusion*)
- In order to survive it should to decrease energy by evaporation of light particles like neutrons, protons and alphas {xn, xp, xa channels and the combination of them}. Excitation functions of xn channels were measured
- High angular momentum decreased by emission of gammas

Experimental setup

Exposition  9.8 s

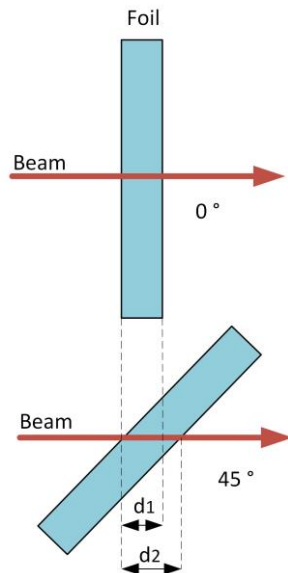
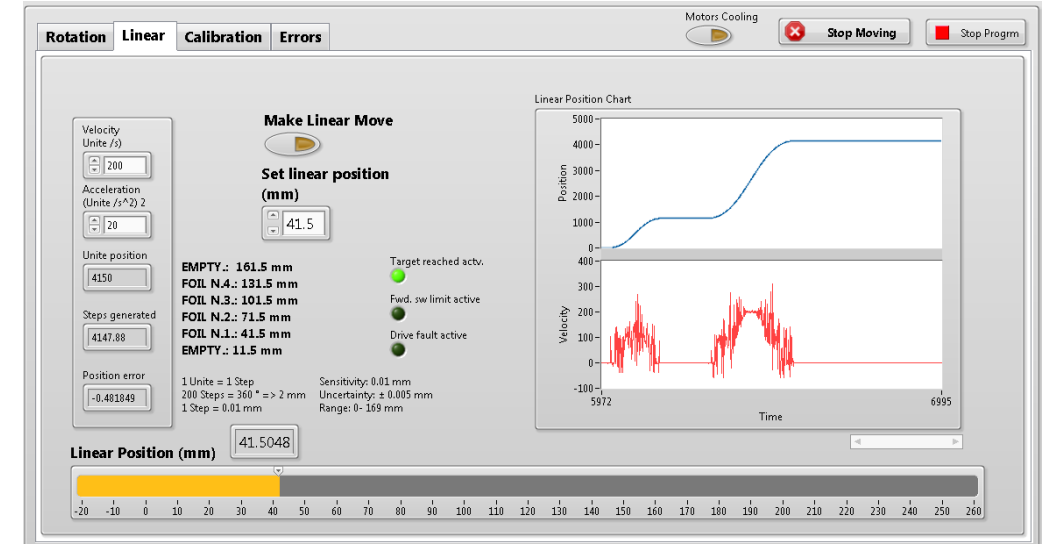
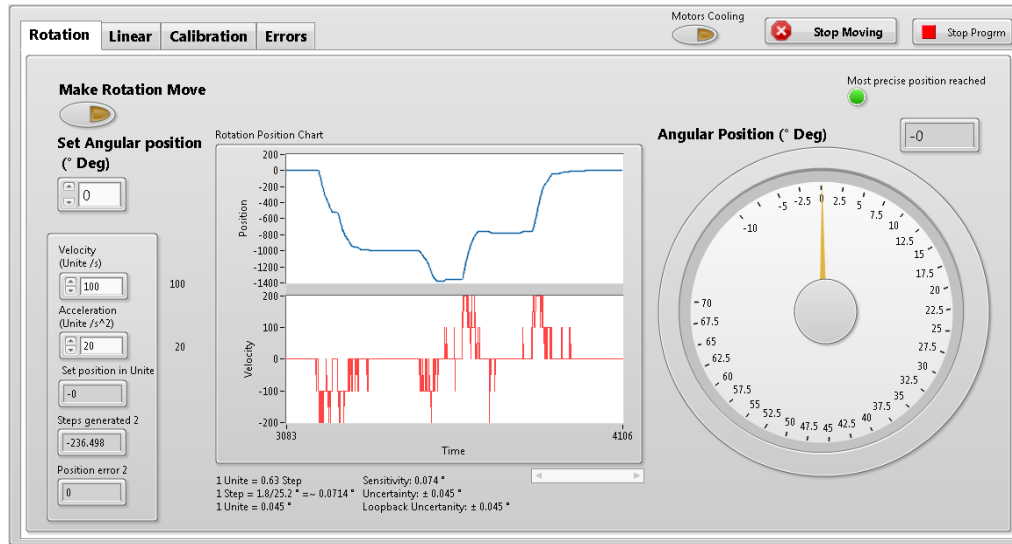
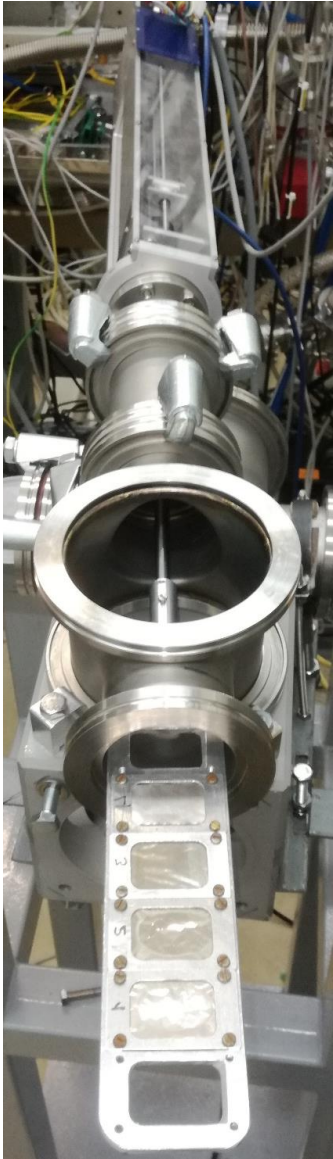


Measurement  9.8 s



- Experiment worked in repetitive cycles 10+10 s and 3+3 s
- Exposition: The ion beam was colliding with the target and evaporation residues was implanting into the Catcher foils
- Measurement: The Catcher foils was unfolded, and neighboring detectors were detecting alpha particles from the decay of implanted evaporation residues

Beam energy degrading

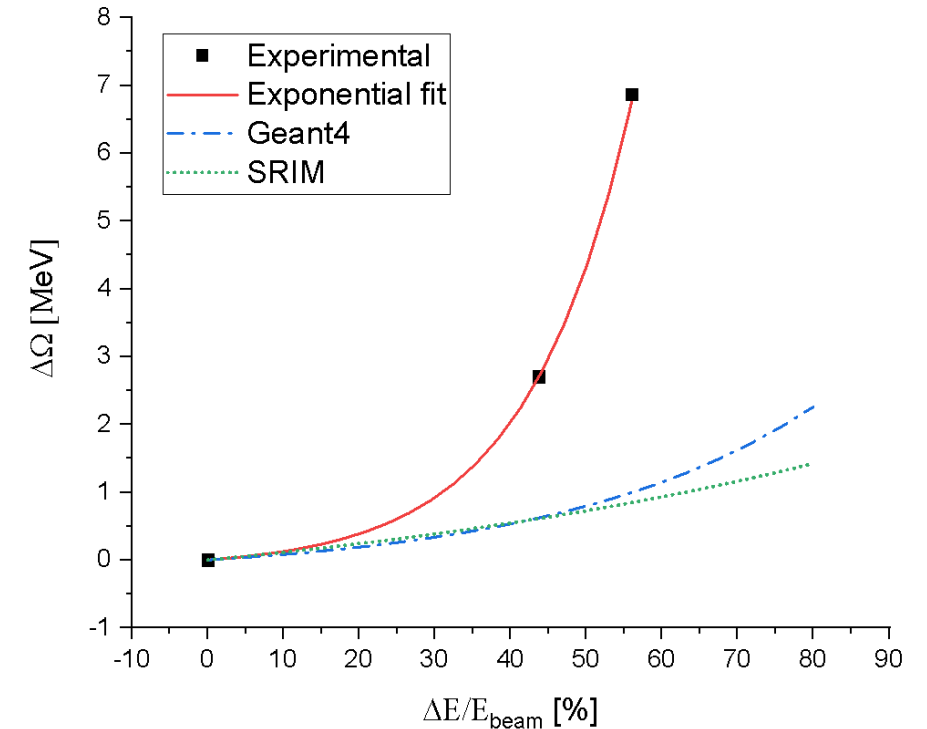
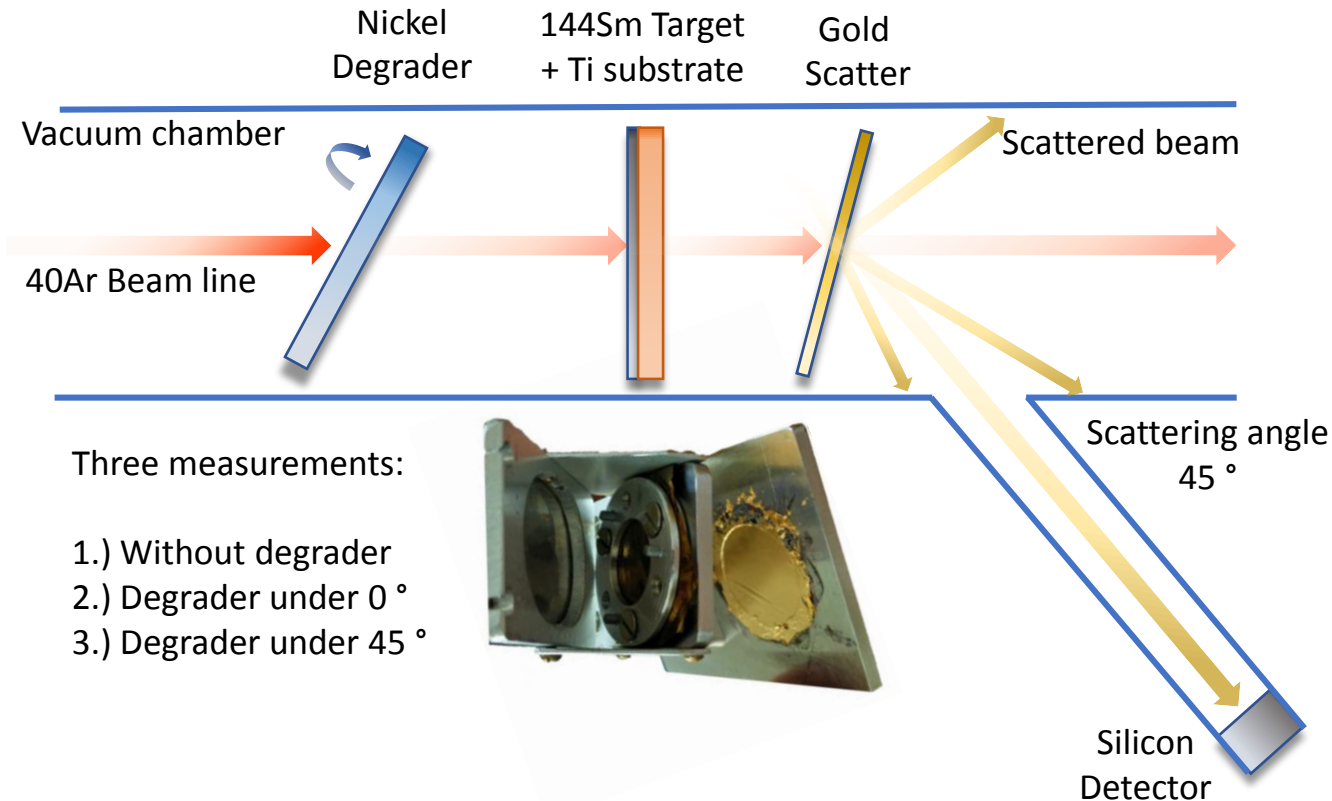


- Degradation foils with different thicknesses were substituted into the beam line
- The beam energy after degradation depends on the energy losses
- Small energy step is optional by the foil rotation
- Degradation mechanism was controlled remotely (closed loop with encoders)
- Desired energy was set and kept stable until alpha detectors collect enough data
- Excitation functions were measured at different energies (E_{lab} 140-240 MeV)

Energy straggling of the beam after degradation

- Energy loss straggling theoretical calculations usually don't match experimental data [1]
- Therefore, the experimental data of energy distribution in the target were measured
- Results had shown a significant discrepancy from SRIM and Geant4 modeling
- Obtained spectra were used to estimate beam energy distribution during the experiment

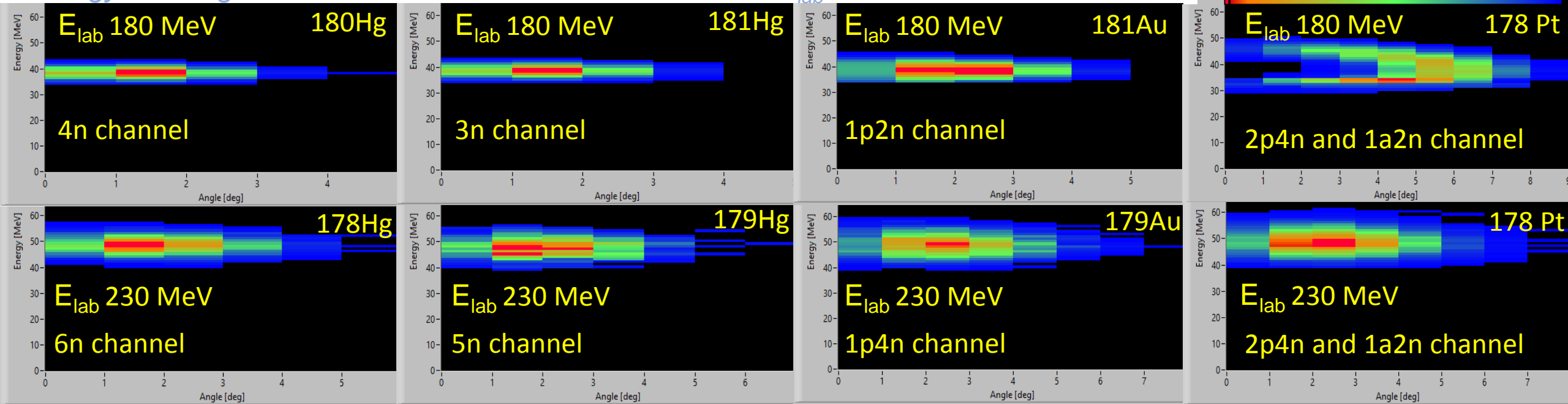
$$\Delta\Omega = \Omega_{straggled} - \Omega_{beam}$$
$$\Delta\Omega = a \left(1 - \exp\left(-b \frac{\Delta E}{E_{beam}}\right) \right)$$
$$b = -0.0727a = -0.1169$$



Energy of residual nuclei

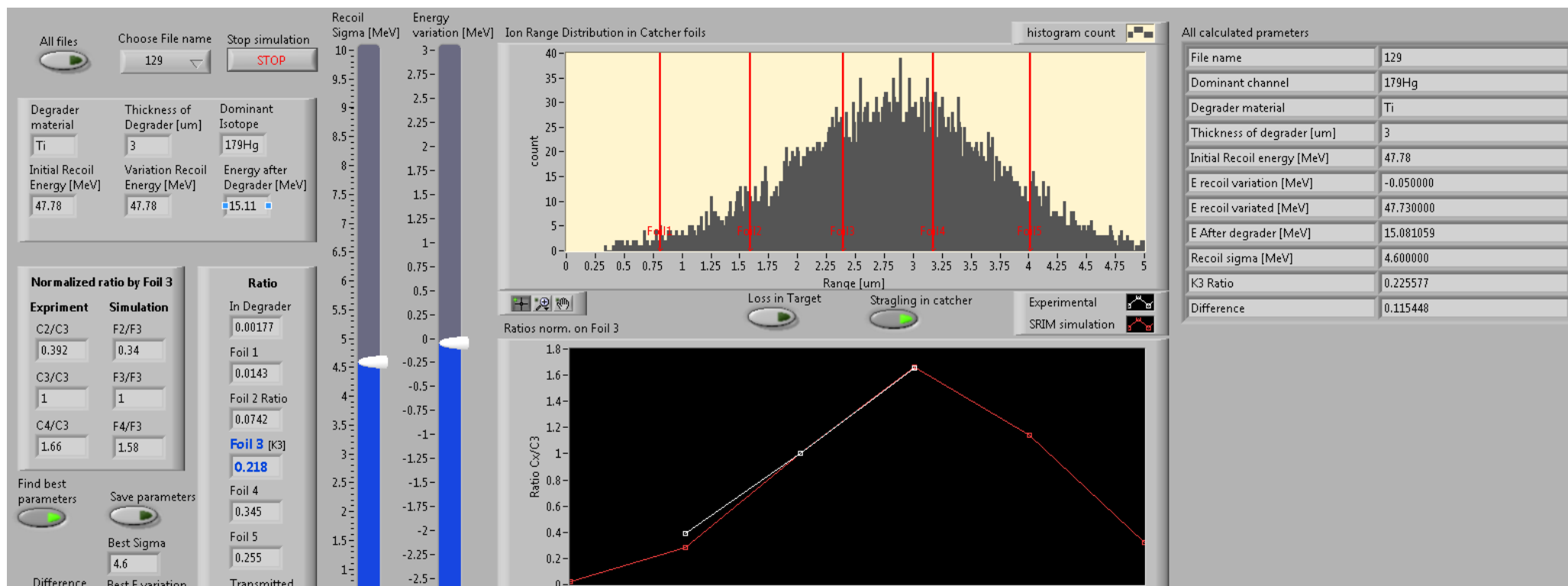
- PACE4 fusion evaporation code was used to calculate energy distribution of residual nuclei [2]
- Only the channels leading to residual nuclei with significant alpha decay were investigated
- Residual nuclei of xn and 1pxn channels had similar parameters under the specific beam energy (E_{lab})
- Angular distribution was similar (2° peak) for all channels across the investigating E_{lab} region (140-240 MeV)
- Energy distribution was getting wider with the higher E_{lab} , but was preserved under the specific E_{lab}
- Some channels lead to the same residual nuclei: like 2p4n and 1a2n \gg 178Pt.
- Alpha channels had significantly split energy distribution under the low angle
- Knowledge of residual nucleus energy is needed to estimate ranges in catcher foils

Energy and angular distribution of residual nucleus under E_{lab} 180MeV and 230 MeV



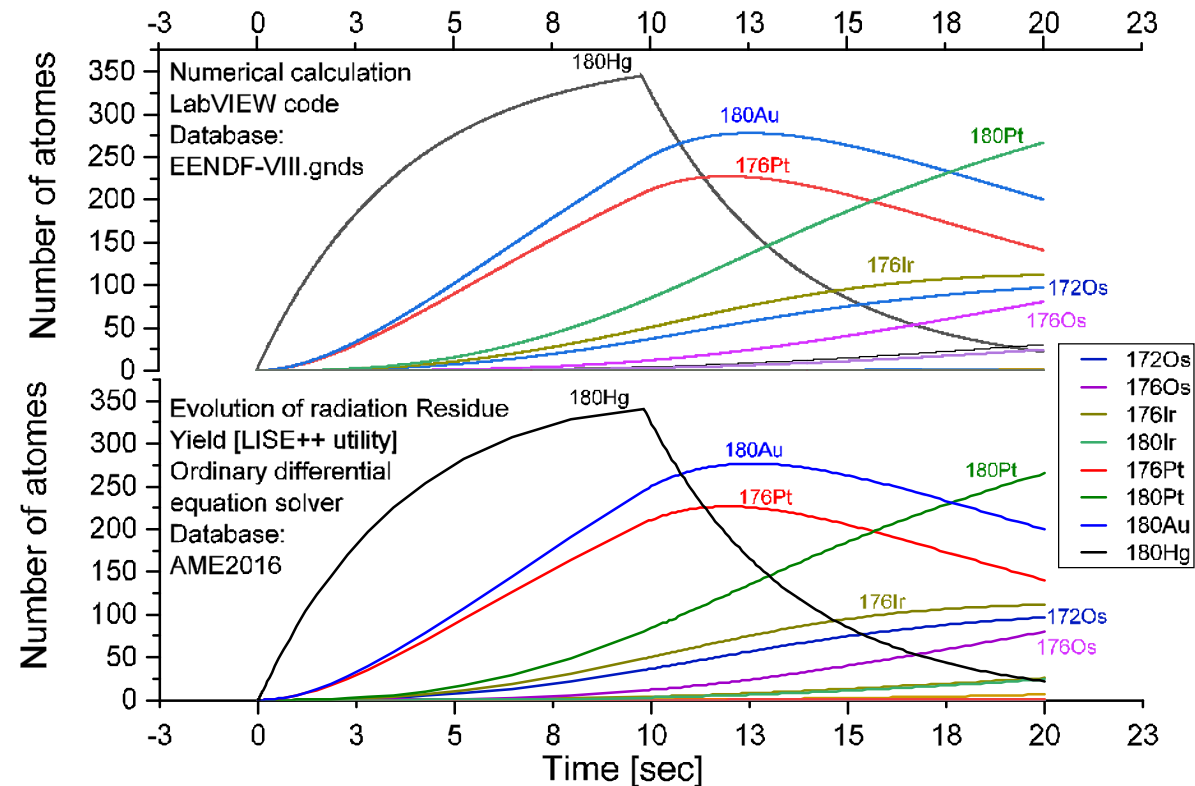
Estimation of ranges in catcher foils

- Energy of residual nuclei was estimated from PACE4 data and the beam distribution in the target
- Simulations of ranges in catcher foils didn't match the experiment well and was probably caused by complexity of energy and angular straggling. Geometrical imperfections like thickness uniformity and rumpeling (of degraders, target, catcher foils itself) cause additional straggling which is unable to simulate.
- Therefore, the several slight variations of calculated energy distribution of residual nucleus were tried to fit the experimental data. For the fast calculation of mean ranges a code based on SRIM tables [3] was designed.
- Experimental yields from foils № 2, 3, 4 were used for range distribution estimation

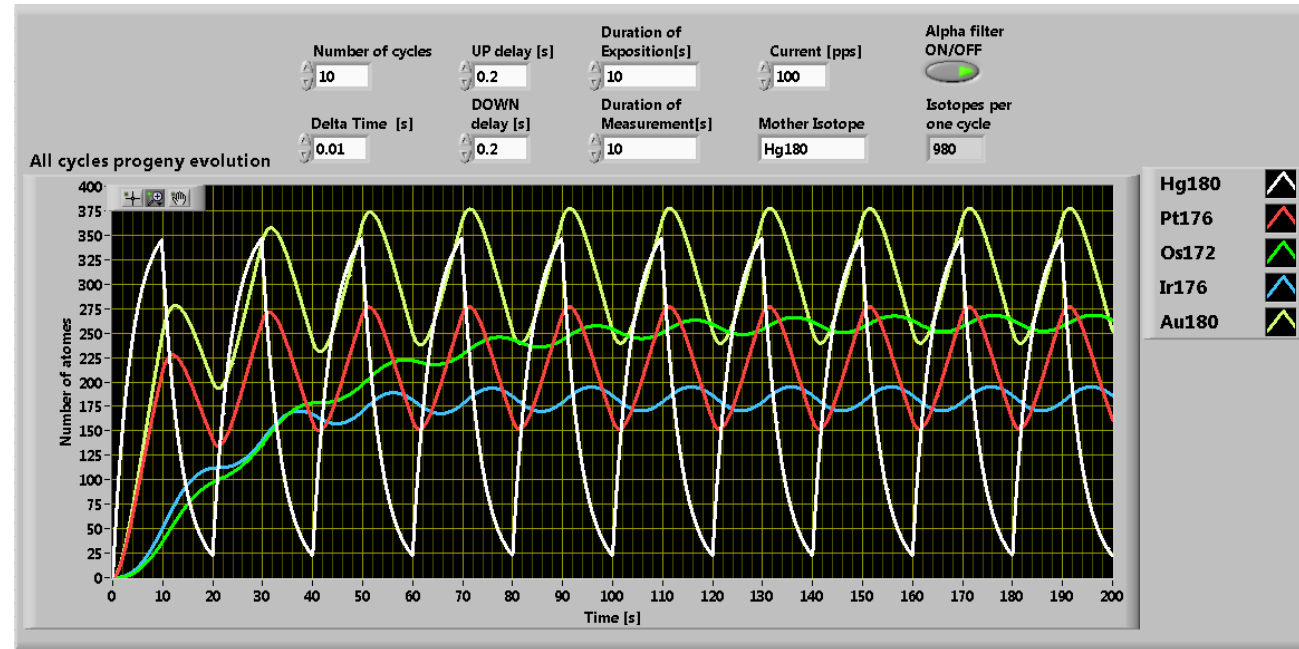


Decay progeny of residual nucleus

- Code for decay progeny numerical calculation using ENDF-VIII.gnds decay database was designed
- Algorithm was compared with LISE++ utility for Evolution of radiation residue yield calculation [4],[5]
- Algorithm could calculate optional cycles with defined irradiation and decay times (including movement time)
- Output alpha filter could be set to investigate just progeny with significant alpha decay



Calculation of 180Hg progeny for current 100ppt, irradiation 9.8 s, decay 10.2 s. Results from both codes are identical.

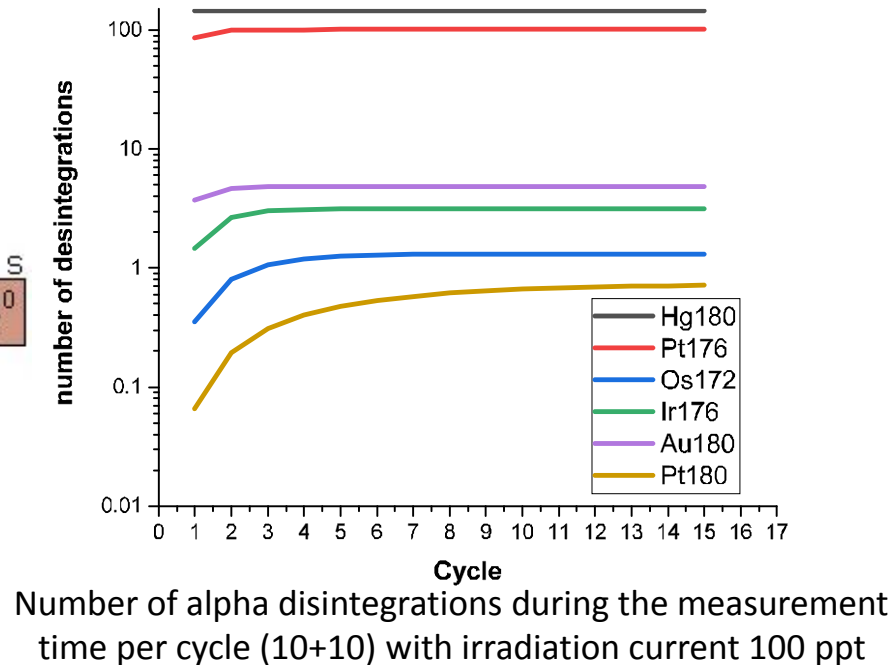
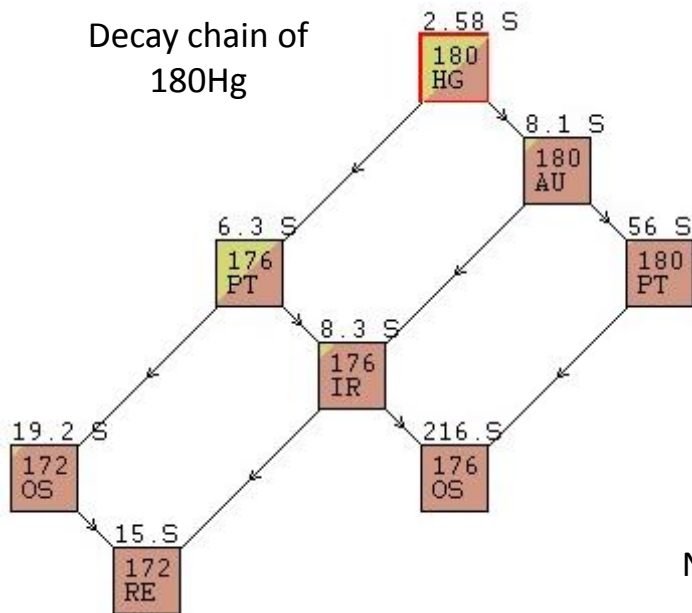
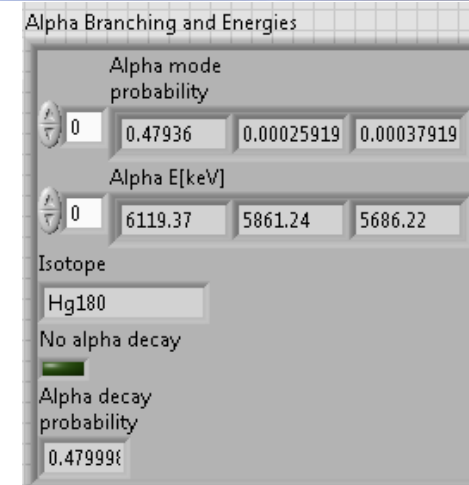


Calculation via numerical LabVIEW code of 180Hg progeny for current 100ppt, irradiation 9.8 s, decay 10.2 s with 10 repetitive cycles

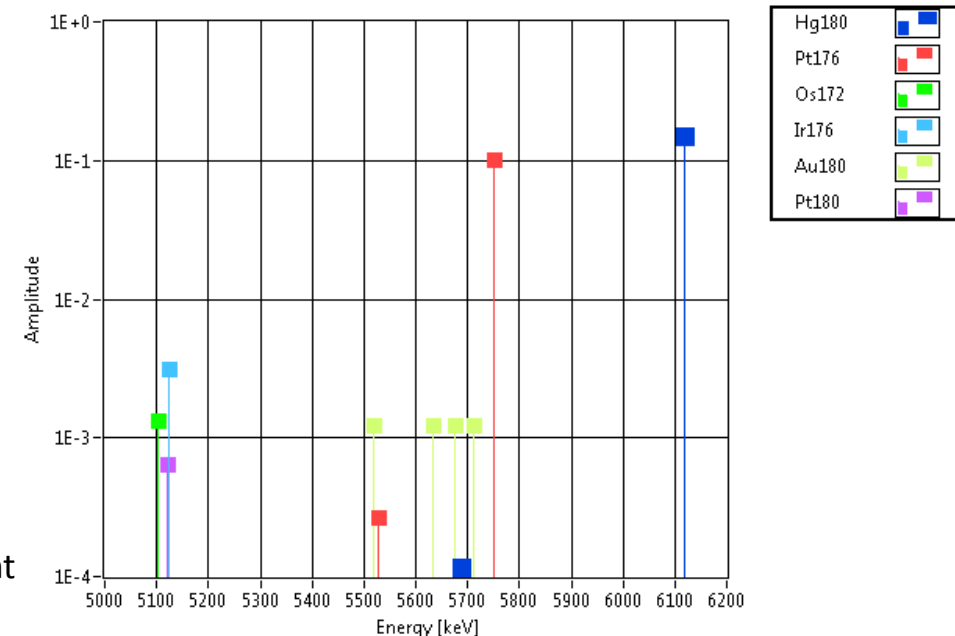
- Evolution shows that equilibrium is reached at ~8th cycle

Normalization of alpha decay amplitudes on one disintegration of mother isotope

- All investigated residual nuclei decay progenies established equilibrium during first few cycles
- After the 15th measurement cycle the number of alpha disintegrations was stable and didn't change further
- If the irradiation current is 100ppt then during exposition time 9.8s, 980 isotopes were accumulated
- Amplitude of one disintegration could be simply obtained by division of alpha disintegrations number during measurement time by 980
- Number of disintegrations before equilibrium could be neglected with respect to the high number of cycles during the experiment (~500 cycles per one specific E_{lab}).
- All alpha modes were examined

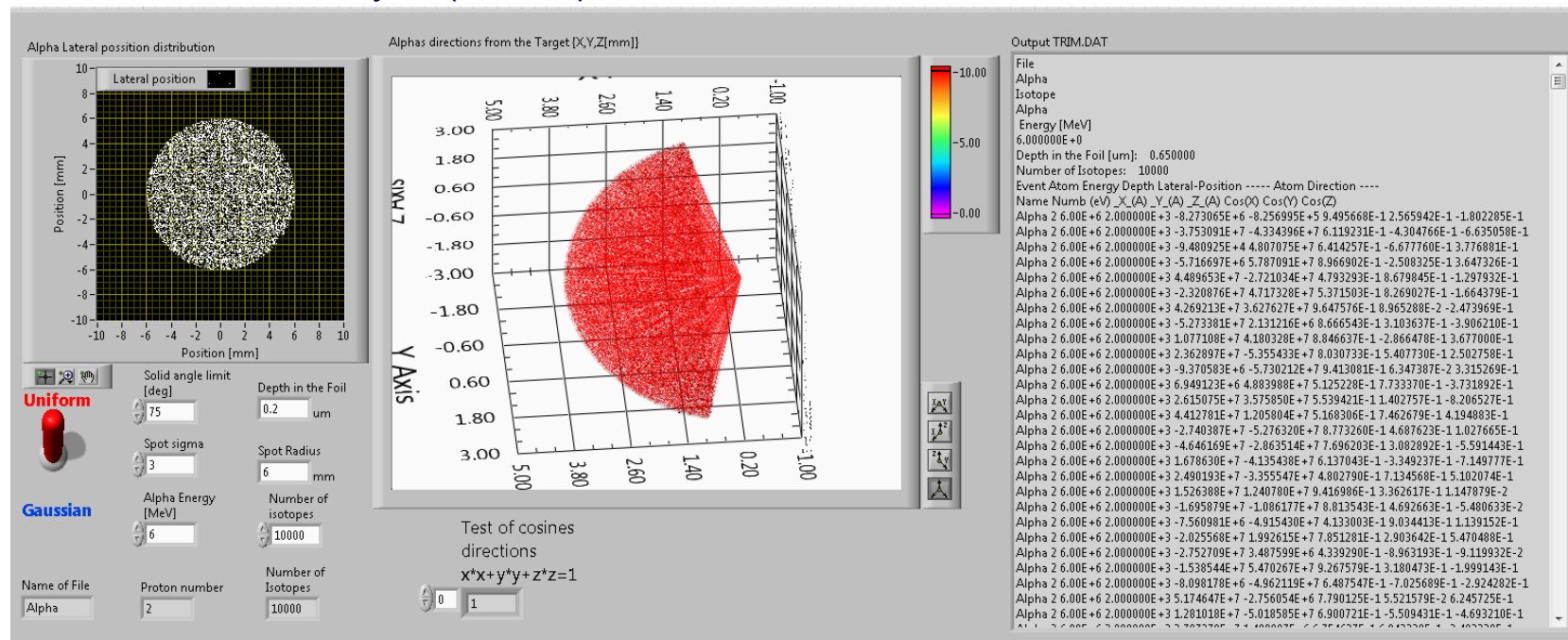


Alpha decay energies and amplitudes for one disintegration of mother isotope

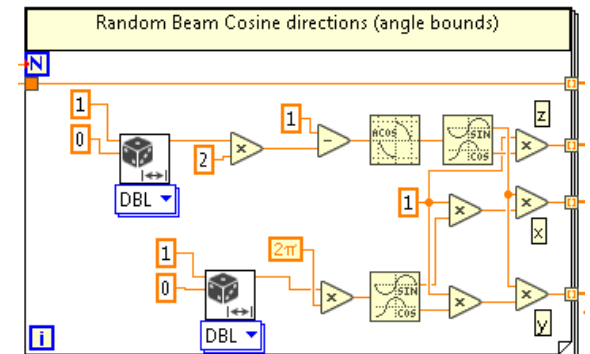
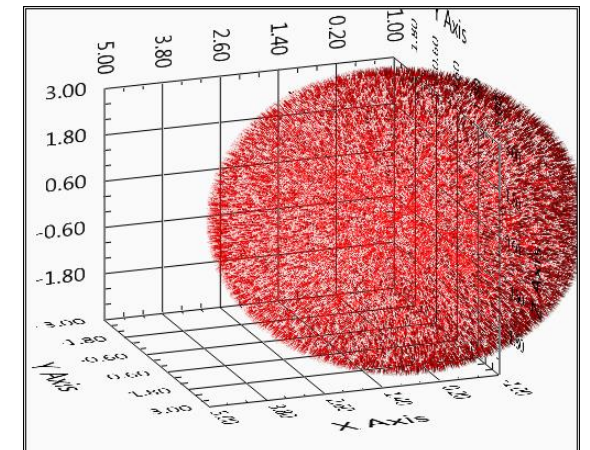


Simulation of the alpha spectra from the catcher foils

- Alpha spectra were simulated in TRIM Monte Carlo code (Transport of Ions in Matter) [6]
- Input parameters were generated via LabVIEW code as TRIM.DAT input file for TRIM simulation
- In order to shorten simulation time the cosine directions of alpha were generated in solid angle 75°
- Simulations were performed for the specific depths (0 - 0.8 μm) inside the catcher foil with the specific alpha energies (3.5 – 7 MeV)
- Simulations were calculated in batch mode (TRIMAUTO) controlled from LabVIEW
- Also silicon dead layer (50 nm) of detector were taken account



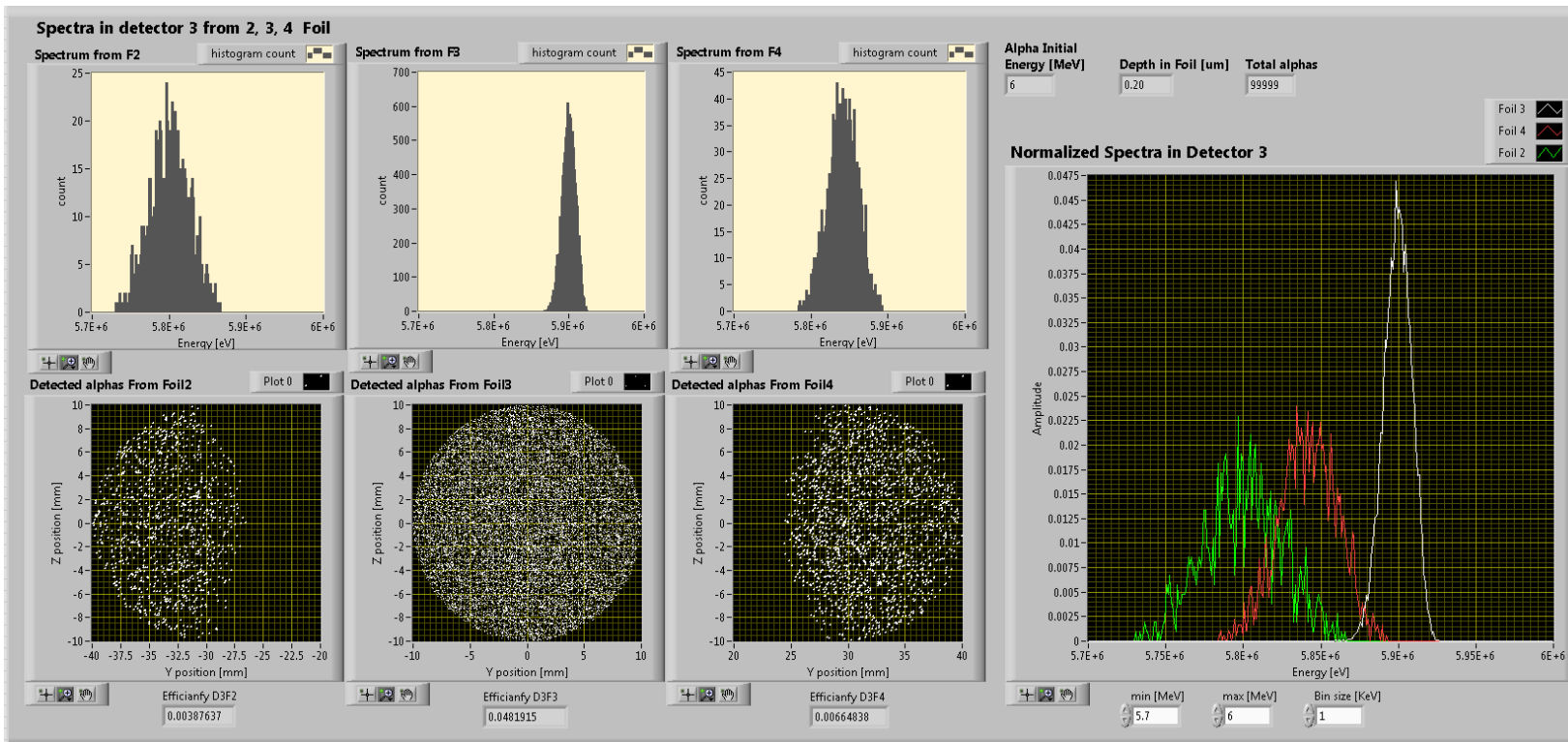
Front panel of code for generating TRIM.DAT input file for TRIM simulation



Algorithm for generation of the uniformly spread cosine directions, to simulate isotropic radiation

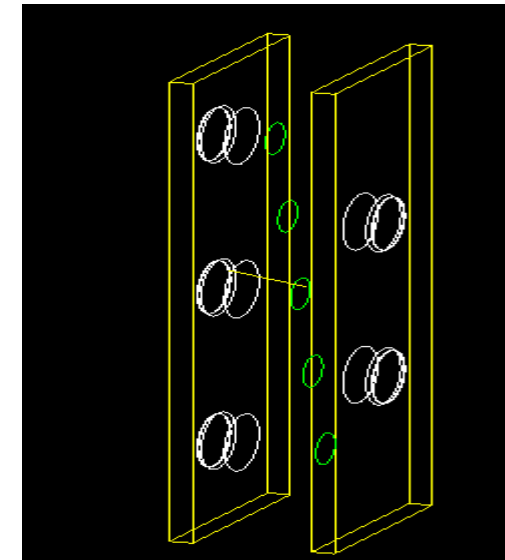
TRIM simulation results projection on geometry of detectors

- Code for TRIM results projection on detectors geometry was designed.
- All simulated spectra in detectors were obtained with respect of collimation by setup construction
- Code also allows to calculate geometric efficiency of detectors.
- Geometric efficiency were also simulated in Geant4 via geantino particle for higher statistics
- Simulations have shown high influence of neighboring foils on detectors



Setup geometry was modeled in Geant4

Table of geometric efficiency of detectors from different foils



	F1	F2	F3	F4	F5
D1	0.0830	0.0033	0	0	0
D2	0.0066	0.0377	0.0049	0	0
D3	0	0.0033	0.0486	0.0059	0
D4	0	0	0.0049	0.0608	0.0014
D5	0	0		0.0059	0.0313

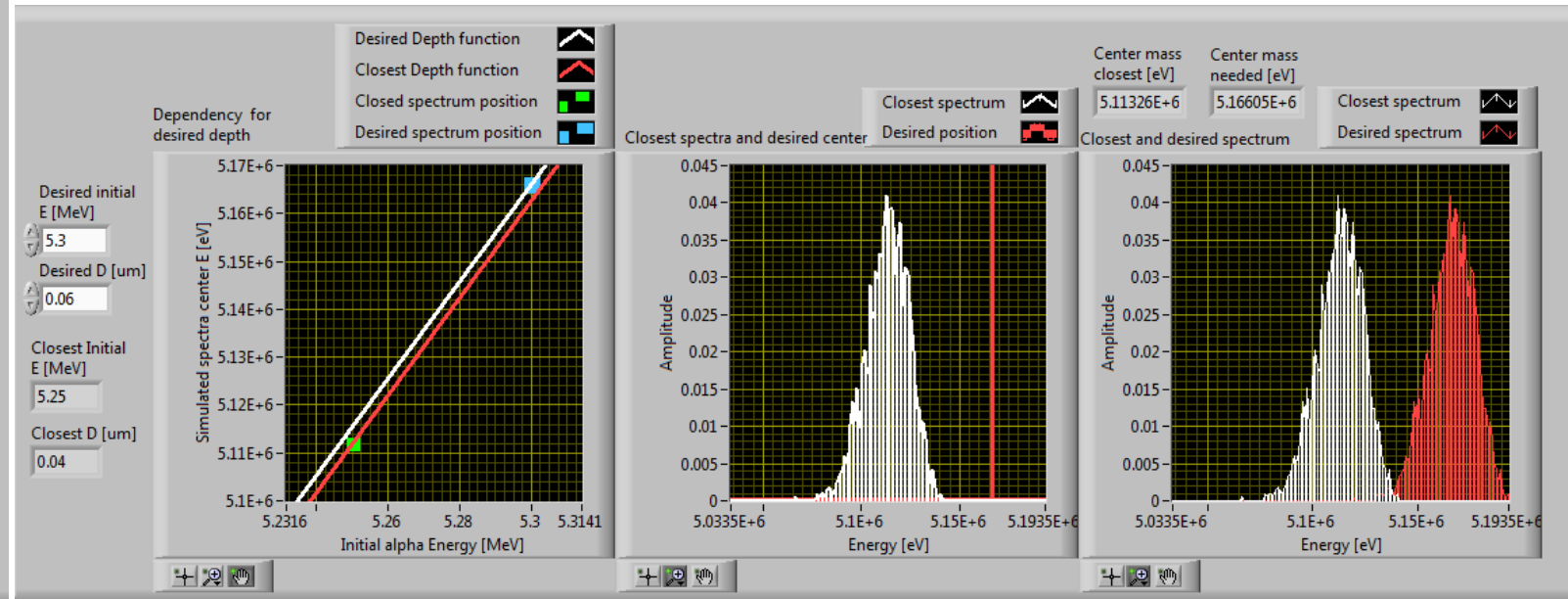
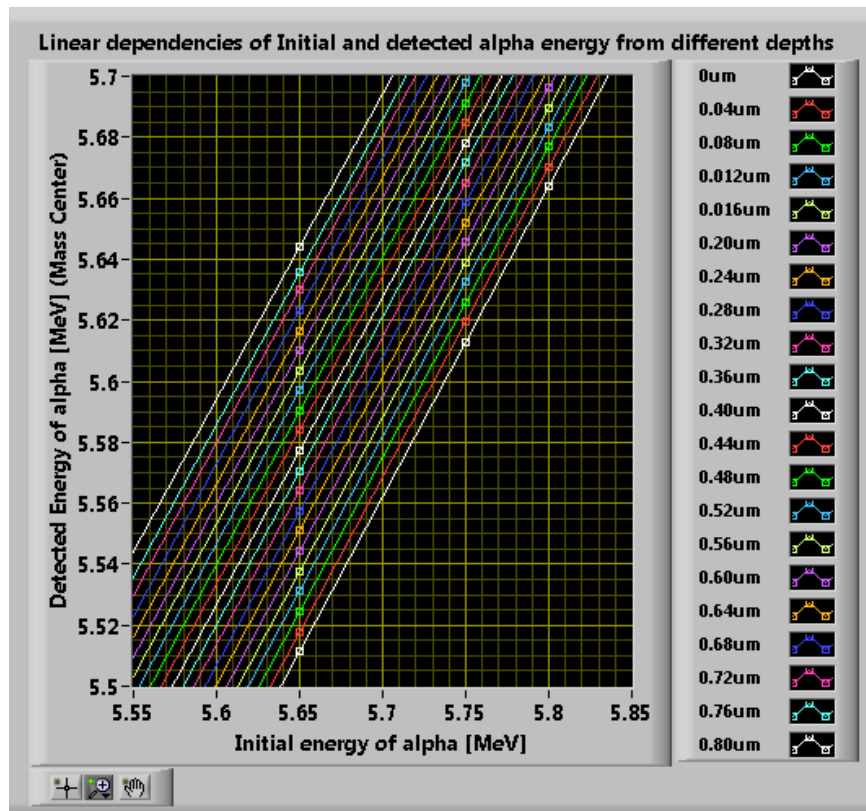
Modeling of spectra in detector for specific residual nuclei

- Simulated alpha spectra were used to model spectra in detector caused by specific residual nuclei
- Initial alpha energy and simulated (mass center energy) from different depths of foil have linear dependencies
- Smooth step of energy and depth was obtained by linear regression and convolution of closest spectrum on calculated position

Position of energy mass center in detector E_{DET} could be calculated for desired depth in foil D and initial alpha energy E_{INI} by formula:

$$E_{DET} = E_{INI} \cdot (D \cdot -0.0193724 + 1.0162) + (D \cdot 0.274099 - 0.230097)$$

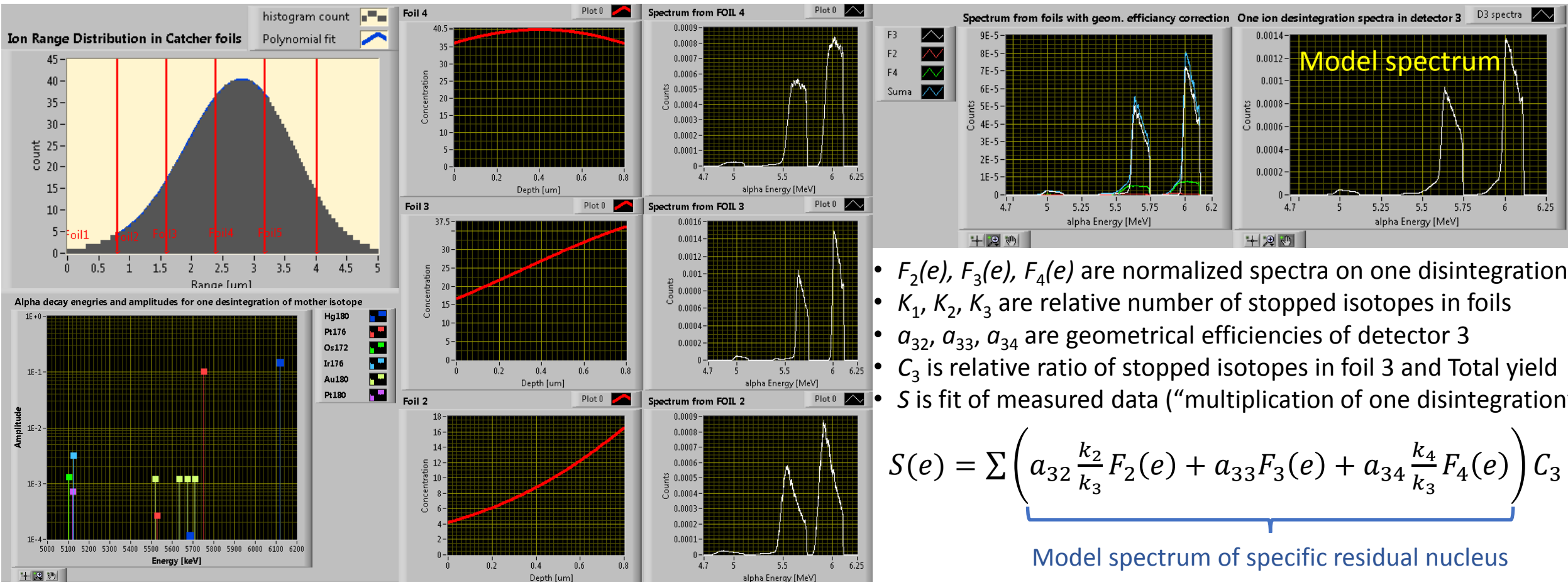
Every combination of detector and foil have different formula, shown one is for detector №3 detecting from foil №3



Convolution of closest spectrum on desired position

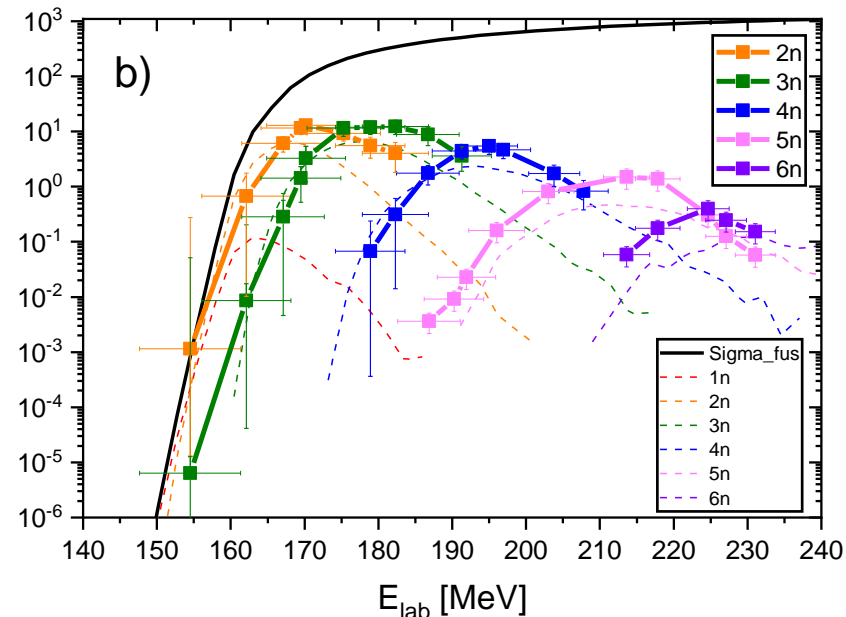
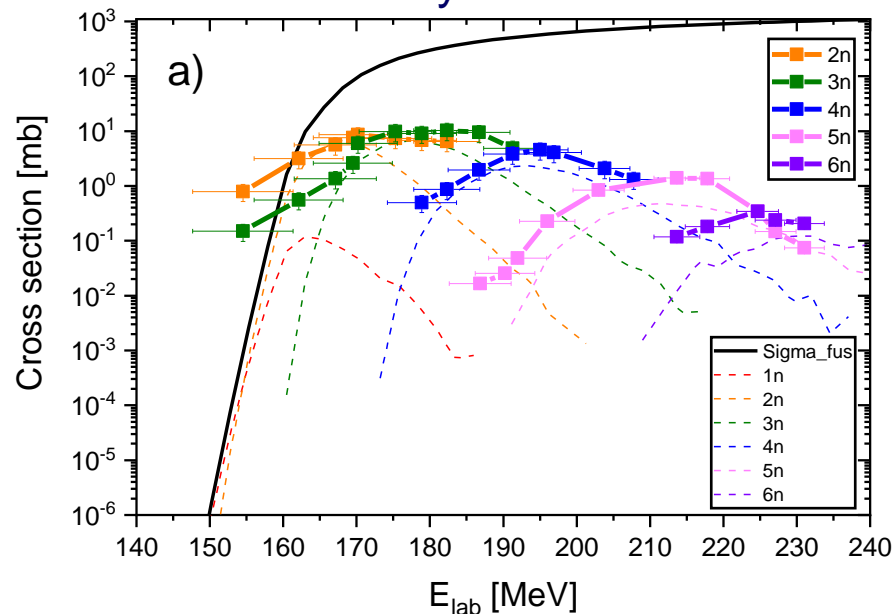
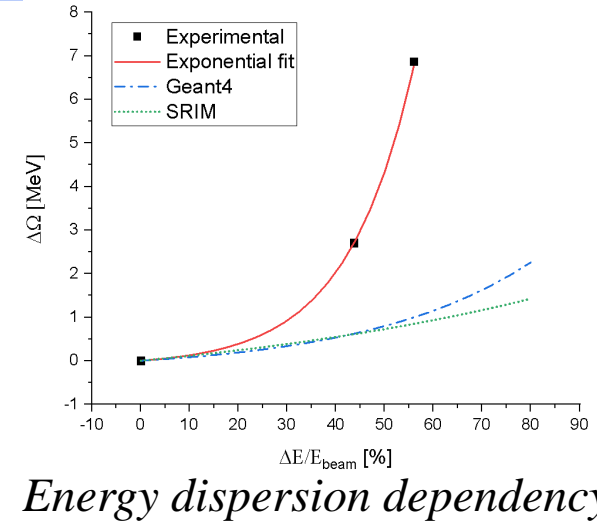
Modeling of spectra in detector for specific residual nuclei

- Calculated alpha lines amplitudes for the residual nuclei were convoluted with simulated spectra in detectors with respect to estimated range distribution in the catcher foils.
- Range distribution of the residual nuclei have strong effect on the final alpha spectrum
- With knowledge of the range distribution and detectors geometric efficiency a final spectrum could be estimated



Correction of excitation functions on energy dispersion

- Energy dispersion $\Delta\Omega$ of the ion beam caused by Nickel degraders rise exponentially with the increasing of energy loss fraction $\Delta E/E_{\text{beam}}$
- Measured cross sections on small energies (close to the fusion barrier) were higher than possible ones, because beam energy E_{lab} was also spread into the E_{lab} region where higher Yield was.
- This effect was corrected by deconvolution of the result excitation functions by energy dispersion.
- After the deconvolution procedure the excitation functions are in higher correlation with theory



Determined cross sections of xn-evaporation channels of the reaction $^{40}\text{Ar} + ^{144}\text{Sm}$ measured by using the catcher foil method (year 2017) a) before and b) after deconvolution. (Dashed lines- NRV channel coupling model)

Conclusion

- Excitation functions of x_n channels were calculated from measured data with sufficient confidence
- Other channels currently are under analysis
- Classical peak fitting was impossible to perform due to complexity of measured spectra
- Fitting by model functions fixed energies and relative amplitudes with respect for decay evolution
- Fitting by model functions with fixed parameters has shown a sufficient solution for complicated spectra

References

- [1] S. Kumar, S. Rani, P. Sharma, S. A. Khan, and P. K. Diwan, “Energy loss and associated parameters in energy spectra of Li, C and O ions in Nickel foils,” Vacuum, vol. 181, no. July, p. 109606, 2020.
- [2] O.B.Tarasov, D.Bazin NIM B 266 (2008) 4657-4664;
A.Gavron, Phys.Rev. C21 (1980) 230-236;
<http://lise.nscl.msu.edu/pace4>
- [3] J. F. Ziegler, M. D. Ziegler, and J. P. Biersack, “SRIM - The stopping and range of ions in matter (2010),” Nucl. Instruments Methods Phys. Res. Sect. B Beam Interact. with Mater. Atoms, vol. 268, no. 11–12, pp. 1818–1823, 2010.
- [4] O.B.Tarasov, D.Bazin NIM B 266 (2008) 4657-4664;
A.Gavron, Phys.Rev. C21 (1980) 230-236;
<http://lise.nscl.msu.edu/pace4>
- [5] The LISE code web sites: <http://www.nscl.msu.edu/lise>
- [6] Biersack, Haggmark A Monte Carlo computer program for the transport of energetic ions in amorphous targets (1980) Nuclear Instruments and Methods, 174, p. 257. Cited 3976 times.
- [7] S. Kumar, P. K. Diwan, and S. Kumar, “Energy loss straggling for α -particles in varying thicknesses of Al, Ti and Ni metallic foils,” Radiat. Phys. Chem., vol. 106, pp. 21–25, 2015.

**Authors thank to internal IGA grant of Palacký University
(IGA_PrF_2020_011).**



Thank you for Your Attention!

НАЦИОНАЛЬНЫЙ ИСЛЕДОВАТЕЛЬСКИЙ ЦЕНТР
Dubna

**Периодическая таблица элементов
Д.И. Менделеева**
D.I. Mendeleev's Periodic Table of Elements

1	2											13	14	15	16	17	18
H 1.00794 Hydrogen	He 4.002602 Helium											B 10.811 Boron	C 12.011 Carbon	N 14.00644 Nitrogen	O 15.9994 Oxygen	F 18.9984032 Fluorine	Ne 20.1797 Neon
Li 6.941 Lithium	Be 9.012182 Beryllium											Al 26.9815385 Aluminum	Si 28.0855 Silicon	P 30.973761508 Phosphorus	S 32.065 Sulfur	Cl 35.453 Chlorine	Ar 39.948 Argon
Na 22.98976928 Sodium	Mg 24.30409 Magnesium	3	4	5	6	7	8	9	10	11	12	Al 26.9815385 Aluminum	Si 28.0855 Silicon	P 30.973761508 Phosphorus	S 32.065 Sulfur	Cl 35.453 Chlorine	Ar 39.948 Argon
K 39.0983 Potassium	Ca 40.078 Calcium	Sc 44.955912 Scandium	Ti 47.88 Titanium	V 50.9415 Vanadium	Cr 51.9961 Chromium	Mn 54.938044 Manganese	Fe 55.845 Iron	Co 58.933194 Cobalt	Ni 58.6934 Nickel	Cu 63.546 Copper	Zn 65.39 Zinc	Ga 69.723 Gallium	Ge 72.61 Germanium	As 74.921595 Arsenic	Se 78.96 Selenium	Br 79.904 Bromine	Kr 83.80 Krypton
Rb 85.4678 Rubidium	Sr 87.62 Strontium	Y 88.90585 Yttrium	Zr 91.224 Zirconium	Nb 92.90638 Niobium	Mo 95.94 Molybdenum	Tc [98] Technetium	Ru 101.07 Ruthenium	Rh 101.0655 Rhodium	Pd 106.42 Palladium	Ag 107.8682 Silver	Cd 112.411 Cadmium	In 114.818 Indium	Sn 118.710 Tin	Sb 121.757 Antimony	Te 127.60 Tellurium	I 126.90547 Iodine	Xe 131.29 Xenon
Cs 132.90545 Cesium	Ba 137.327 Barium	La 138.9055 Lanthanum	Hf 178.49 Hafnium	Ta 180.9479 Tantalum	W 183.84 Tungsten	Re 186.207 Rhenium	Os 190.23 Osmium	Ir 192.22 Iridium	Pt 195.08 Platinum	Au 196.96654 Gold	Hg 200.59 Mercury	Tl 204.3833 Thallium	Pb 207.2 Lead	Bi 208.98037 Bismuth	Po [209] Polonium	At [210] Astatine	Rn [222] Radon
Ra 226.075 Radium	Fr [223] Francium	Ac [227] Actinium	Rf [261] Rutherfordium	Db [262] Dubnium	Sg [266] Seaborgium	Bh [267] Bohrium	Hs [269] Hassium	Mt [270] Meitnerium	Ds [271] Darmstadtium	Rg [272] Roentgenium	Cn [285] Copernicium	Nh [286] Nihonium	Fl [289] Flerovium	Mc [290] Moscovium	Lv [293] Livermorium	Ts [294] Tennessine	Og [294] Oganesson
Lanthanides																	
Ce 140.12 Cerium	Pr 140.90765 Praseodymium	Nd 144.242 Neodymium	Pm [145] Promethium	Sm 150.36 Samarium	Eu 151.964 Europium	Gd 157.25 Gadolinium	Tb 158.92534 Terbium	Dy 162.50 Dysprosium	Ho 164.93032 Holmium	Er 167.26 Erbium	Tm 168.93421 Thulium	Yb 173.04 Ytterbium	Lu 174.967 Lutetium	H 1.00794 Hydrogen			
94	Am [243] Americium	95	Cm [247] Curium	96	Bk [247] Berkelium	97	Cf [251] Californium	98	Es [252] Einsteinium	99	Fm [257] Fermium	100	Md [258] Mendelevium	101	Nr [259] Nobelium	102	